Applied Surface Science 410 (2017) 111–116

Contents lists available at ScienceDirect

Applied Surface Science

journal homepage: www.elsevier.com/locate/apsusc

Full Length Article

Towards the atomic-scale characterization of isolated iron sites confined in a nitrogen-doped graphene matrix

Qingfei Liu[a,b], Yun Liu[a,b], Haobo Li[a,b], Lulu Li[c], Dehui Deng[a], Fan Yang[a,*], Xinhe Bao[a,*]

[a] State Key Laboratory of Catalysis, CAS Center for Excellence in Nanoscience, Dalian National Laboratory for Clean Energy, Dalian Institute of Chemical Physics, Chinese Academy of Sciences, Dalian, 116023, China
[b] University of Chinese Academy of Sciences, Beijing, 100039, China
[c] College of Chemistry, Faculty of Chemical, Environmental and Biological Science and Technology, Dalian University of Technology, Dalian, 116023, China

ARTICLE INFO

Article history:
Received 16 February 2017
Received in revised form 8 March 2017
Accepted 9 March 2017
Available online 10 March 2017

Keyword:
Ball-milling
AFM
STM
Nitrogen-doped graphene
Isolated iron sites

ABSTRACT

Atomic scale characterization of the surface structure of powder catalysts is essential to the identification of active sites, but remains a major challenge in catalysis research. We described here a procedure that combines atomic force microscopy (AFM), operated in air, and scanning tunneling microscopy (STM), operated in UHV, to obtain the atomic structure and local electronic properties of powder catalysts. The atomically dispersed Fe-N-C catalyst was used as an example, which was synthesized by low temperature ball milling methods. We discussed the effect of solvents in the dispersion of powder catalysts on a planar support, which is key to the subsequent atomic characterization. From the morphology, atomic structure and local electronic properties of the Fe-N-C catalyst, our combined measurements also provide an insight for the effect of ball milling in the preparation of atomically dispersed metal catalysts.

1. Introduction

Highly dispersed metal atoms or sub-nanometer clusters confined on a solid support could often demonstrate superb catalytic activity and selectivity in chemical reactions [1–4], which has led to a general interest in catalysis and chemical research. The design and synthesis of these atomically dispersed catalysts have thus been suggested as an effective strategy to develop highly efficient, yet cost-effective catalyst that could meet with our current energy and environmental needs [5]. However, there are very few techniques that can resolve the structural and electronic properties of these metal centers or clusters at the atomic level, which has hampered our understanding and thus the design of these atomically dispersed supported catalysts.

Transmission electron microscopy (TEM) has often been used to resolve the structure of the above mentioned catalysts. But a few drawbacks were also mentioned that the technique is not sensitive to surface structure and could modify small metal clusters while imaging due to the beam damage. Scanning tunneling microscopy (STM), a nondestructive imaging technique, could avoid these problems, but were rarely employed to study powder catalysts [4], because of its sensitivity to atomic contaminants and the difficulty in characterizing samples with high surface corrugations. In this case, atomically dispersed metal catalysts, when properly treated and dispersed on a planar surface, could be suitable for STM characterization. Here, we report the combination of atomic force microscopy (AFM) and STM methods to achieve atomic-scale characterization of atomically dispersed metal catalysts. AFM operated under the ambient environment allows the quick examination of the dispersion of powder catalyst on a planar support, as well as the morphology and mechanic properties of the catalyst sample. On this basis, STM on the well-dispersed sample surface could readily resolve further the atomic structure and local electronic property. In this paper, we report a study on the Fe-N-C catalyst, which consists of graphene nanosheets (GNs) modified by Fe and N atoms. While inorganic oxides such as alumina and silica were conventionally used as the catalyst support, carbon-based materials have emerged in recent years and exhibit excellent catalytic performance in both thermo- and electro-catalysis [6,7], when the carbon matrix is doped with main group heteroatoms and metal centers. Substitutional doping of heteroatoms, such as N or B, in the carbon matrix is considered a requirement to anchor the active metal center and tune its reactivity [8]. The efforts to synthesize isolated metal centers embedded in a graphene matrix have been tremendous. Typically, pyrolysis [7,9,10] or ball milling [1] methods were used to prepare the Fe-N-C catalyst, while the former

* Corresponding authors.
E-mail addresses: fyang@dicp.ac.cn (F. Yang), xhbao@dicp.ac.cn (X. Bao).

http://dx.doi.org/10.1016/j.apsusc.2017.03.090
0169-4332/

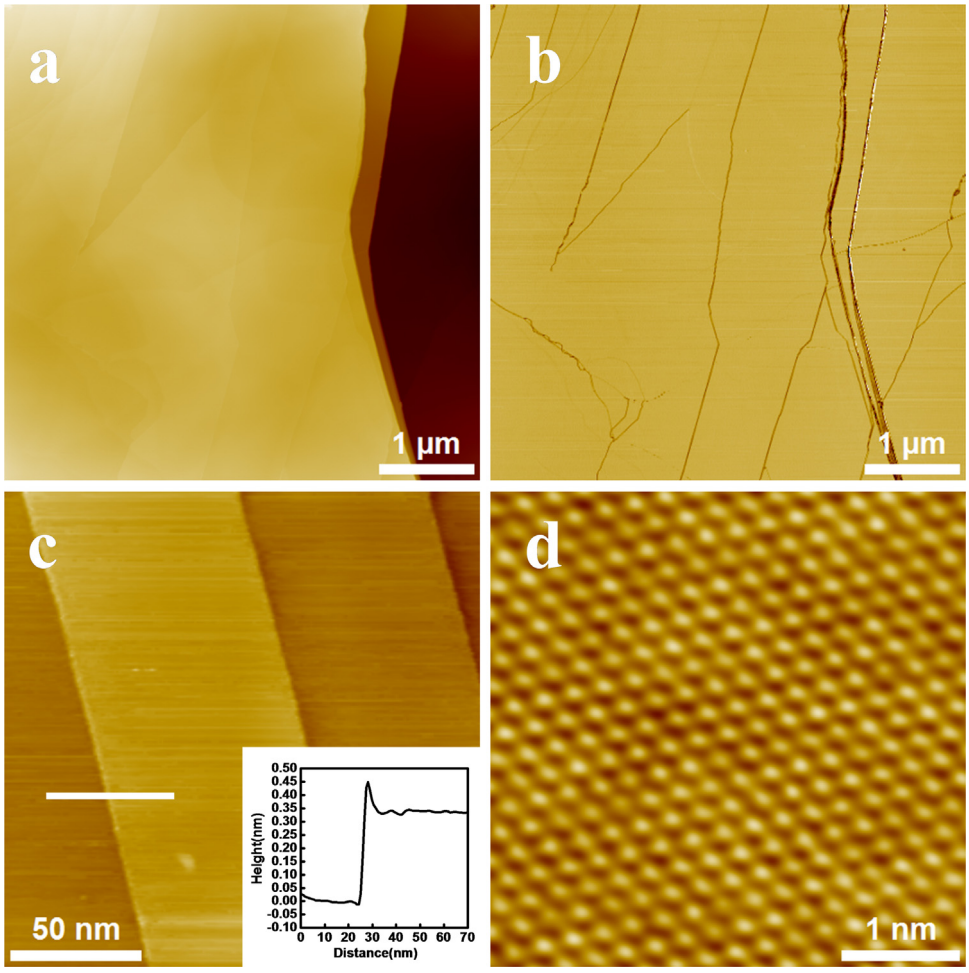

Fig. 1. AFM and STM images of the HOPG substrate. Height and phase images of the same area of HOPG could be obtained simultaneously by typical tapping mode AFM and displayed in (a) and (b), respectively. (c) is the constant current STM image of HOPG. The step height of HOPG is about 3.3 Å, corresponding to monoatomic step height of HOPG. Inset shows the step height of HOPG. (d) shows the atomic resolution STM image of HOPG.

method could often produce metal nanoparticles because of the high temperature treatments involved.

Ball milling, as a low temperature preparation method, has made significant progress in catalyst synthesis in recent years. In addition to its application in preparing catalytic nanomaterials, ball milling has also been used for facilitating chemical reactions, leading to the development of a research area, termed as mechanochemistry [11,12]. How ball milling affects nanomaterial synthesis, however, still requires an atomic level understanding on the ball-milled catalysts. Using the Fe-N-C catalyst as an example, we discuss the effect of ball milling in the synthesis of GN-based nanocatalysts and described a procedure to obtain the surface structure and electronic properties of the Fe-N-C catalyst, which should be generally applicable for the characterization of powder catalysts.

2. Experimental

The preparation of the Fe-N-C catalyst has been described in details in our previous work [1]. Briefly, the sample was prepared by high-energy ball milling of the mixture of iron phthalocyanine (FePc) and GNs, where the mass fraction of FePc is 15%. GNs were obtained by ball milling the graphite flakes (GFs, 99.8%, Alfa Aesar) as described previously [13]. For AFM and STM characterization, the synthesized Fe-N-C catalyst was diluted by petroleum ether or methanol solution at the concentration of 0.1 g/L. After ultrasound sonication, drops of the solution were casted onto a freshly cleaved highly-oriented pyrolitic graphite (HOPG) substrate (1cm × 1 cm; ZYA grade, NT-MDT) by the pipette. The liquid droplet covered the entire surface area of HOPG. HOPG was chosen as the support because: a) it exhibits atomically flat terraces suitable for scanning probe characterization. b) it is easy to obtain a clean HOPG surface using Scotch tape.

After the vaporization of solvent, the HOPG sample was transferred to AFM or STM for characterization. The HOPG sample on the sample plate was marked by a grid with ~3 mm interval, such that AFM and STM tips could be positioned at approximately the same surface area. Tapping-mode AFM measurements were conducted using a Bruker Metrology Nanoscope III-D atomic force microscrope operated under ambient conditions. Commercial tapping mode tips made of phosphorus(n) doped Si were supplied from Veeco with 115–135 μm long cantilevers, with resonance frequencies of 293–387KHz and spring constants of 20–80N/m. After AFM measurements, the sample was transferred into a Createc low-temperature STM system, which is operated under ultrahigh vacuum (UHV). The base pressure of the STM chamber is below 4×10^{-11} mbar and an electrochemically etched W tip was used for STM measurements. STM images, as well as scanning tunneling spectroscopy (STS), were taken at liquid nitrogen (LN_2) or liquid helium (LHe) temperatures and processed using the SPIP software from Image Metrology.

3. Results and discussion

The fresh HOPG surface prepared by Scotch tape is flat with terrace width ranging from a few ten nm to over a hundred nm (Fig. 1). In AFM images, both the height image (Fig. 1a) and the phase image (Fig. 1b) give the clear height difference among the different surface carbon layers. The step heights of HOPG are measured to be 3.3 Å, which is consistent in AFM and STM measurements. Atomically resolved STM images of HOPG (Fig. 1d) shows an ordered hexagonal lattice, with a lattice constant at 2.4 Å, suggesting only half of the surface carbon atoms were resolved as bright protrusions. This is consistent with previous study [14] that the electronic states of carbon atoms, which are located right on top of carbon atoms at the lower layer, are moved away from the Fermi level. Only carbon atoms, located above the center of the hexagonal carbon ring in the second layer, could be resolved as protrusions in the STM.

The selection of solvents was found key to the dispersion of the catalyst sample. Two types of solvents, petroleum ether and methanol, were used to examine the effect of solvents in the dispersion of the Fe-N-C catalyst on HOPG. Fig. 2 shows typical AFM images, which compare the dispersion of the Fe-N-C catalyst after drop casting the methanol or petroleum ether solution on HOPG. Fig. 2a and 2b show the methanol solution deposits some bright protrusions, which were distributed randomly on HOPG. In contrast, the petroleum ether solution leaves large nanoflakes on the HOPG surface (Fig. 2c–d). In the phase images, the morphology of deposited sample could be easily distinguished from the HOPG substrate, since the mechanic properties of the deposited sample is drastically different from that of HOPG.

Note that, the Fe-N-C catalyst is derived from ball milling the mixture of FePc precursors and GNs. One would expect flake-like structures when the catalyst was deposited on HOPG. As petroleum ether could distribute graphene sheets homogeneously on HOPG, methanol solution shows poor solubility for GNs and thus fails the dispersion of the Fe-N-C catalyst. Thus, we expect nonpolar solvents or solvents with low polarity index are suitable for the dispersion of GN-based catalyst. The polarity of dispersion solvents is vital for the deposition of catalyst sample on HOPG.

Using petroleum ether as the dispersion solvent, we then investigated the surface morphology of the Fe-N-C catalyst, as a function of its deposition amount on HOPG. Fig. 3 shows clearly that the surface coverage of GN flakes increases with the increasing numbers of droplets that were casted onto HOPG. We found that GNs tend to disperse homogeneously on HOPG, rather than stacking onto each other, at the initial stage of deposition. As GNs gradually cover almost the entire HOPG surface (Fig. 3c–d), the dispersion of overlayer GNs remains homogenous, rendering a relatively flat surface suitable for scanning probe characterization. When HOPG is fully covered by a few layers of GNs (Fig. 3e–f), bright mounds with

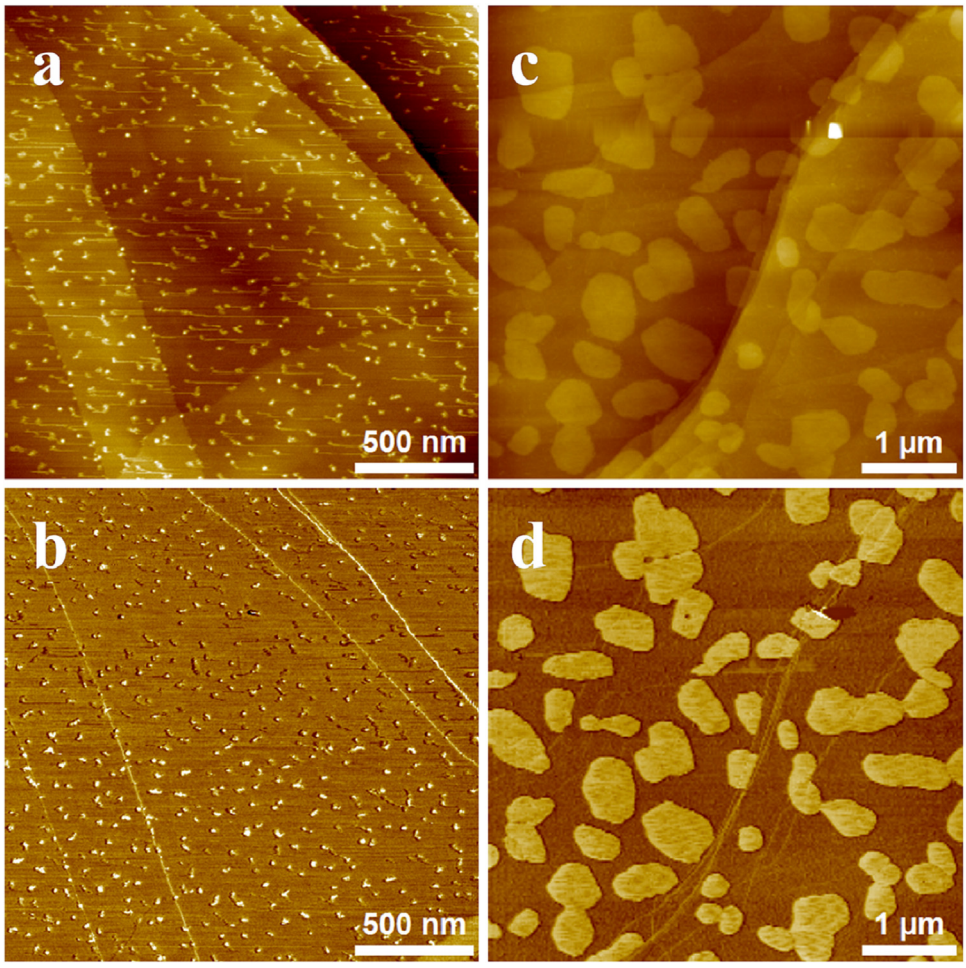

Fig. 2. Effect of solvents on the dispersion of the Fe-N-C catalyst on HOPG. Methanol or petroleum ether were used to disperse the Fe-N-C catalyst and tapping mode AFM were used to characterize the drop-casted Fe-N-C catalyst on HOPG in (a–d). (a) and (b) display height and phase images of the same area after the catalyst was dispersed by methanol and casted onto HOPG. Bright protrusions could be observed and distribute homogeneously on HOPG. (c) and (d) display height and phase images of the same area after the catalyst was dispersed by petroleum ether and casted onto HOPG. Graphene nanosheets were found to deposit homogeneously on the HOPG substrate.

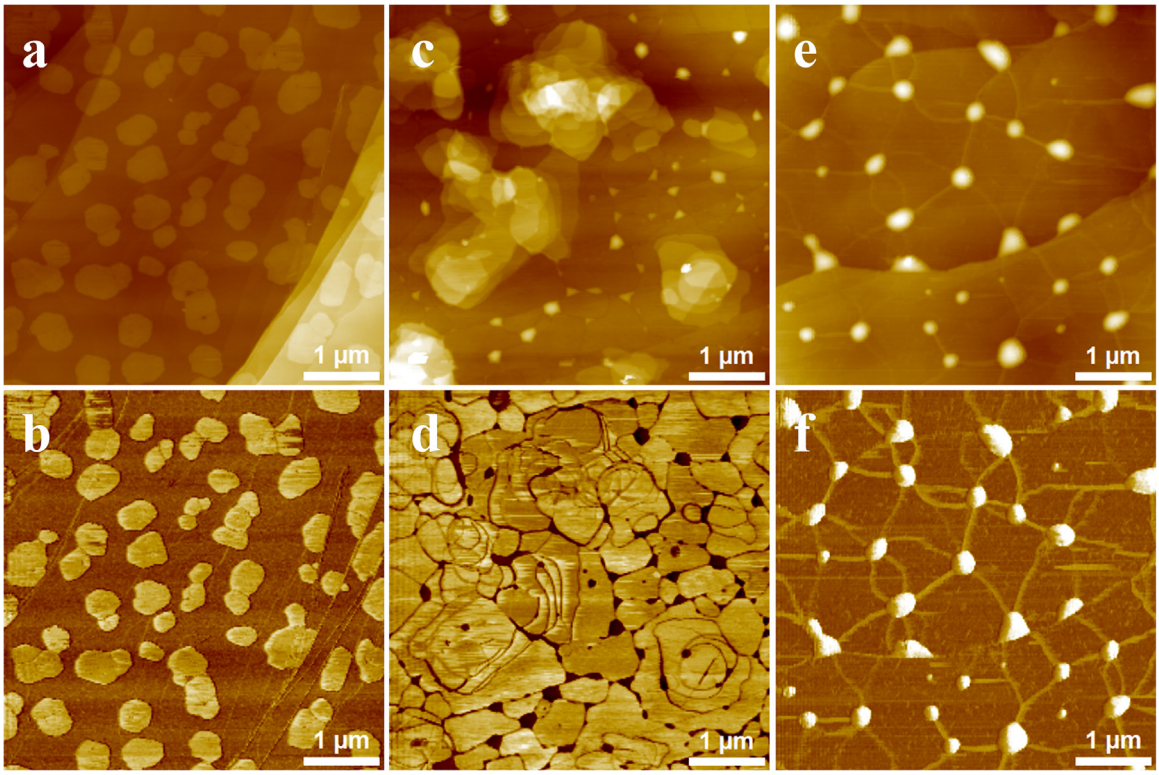

Fig. 3. Surface morphology of the drop-casted Fe-N-C catalyst on HOPG as a function of deposition amount. The corresponding surfaces of HOPG after the deposition of petroleum ether solution, containing Fe-N-C catalysts, were characterized by tapping mode AFM. (a), (c) and (e) display height images of the surfaces casted with 12 μL, 24 μL or 60 μL solution. (b), (d) and (f) show the corresponding phase images of (a), (c) and (e), respectively. All images have the same size at 5 μm × 5 μm. Graphene nanosheets (GNs) tend to disperse homogeneously on HOPG at the initial stage of deposition. The HOPG substrate is almost covered by the stacks of GNs in (c) and fully covered by multilayers of GNs in (e).

a width around 10–20 nm could also be observed at the domain boundaries of GNs.

We checked over the HOPG surface after the solution deposition and found a similar dispersion of GNs across the whole surface. Subsequently, the sample of Fig. 3a was transferred into the UHV chamber for STM characterization at cryogenic temperatures. Fig. 4 shows the morphology and structure of the Fe-N-C catalyst deposited on HOPG. The formation of wrinkles on GN (Fig. 4a) is a typical character of the solution deposited sample. In our sample, wrinkles can be caused by the evaporation of trapped solvent molecules upon deposition. The structure of wrinkles formed on the graphene sheet has been studied in details previously [15,16].

On the planar surface of GN, bright dots could be observed which distribute randomly on the surface and shows a higher density around the wrinkle. Fig. 4b shows the atomic structure of a bright dot. To rule out the possible contamination adsorbed on HOPG, the sample has been annealed in UHV prior to STM characterization. We further used tip manipulation trying to see whether the bright spot could be removed as the tip approached the surface. But these bright dots remained stable during manipulation or under harsh scanning conditions. From bias-dependent STM images (Fig. 4b–d), the apparent heights of these bright dots did not show drastic differences, indicating that the electronic structure of the bright dots are strongly hybridized with that of the graphene matrix, such that the local density of states (LDOS) at the bright spots are continuous at near the Fermi level. In another word, the bright spot appears embedded in the graphene lattice, i.e. the introduction of substitutional heteroatoms. Around the bright dot, the neighboring atomic spots also appear brighter, indicating the modification of electronic structure at neighboring sites.

Besides the structural characterization, LDOS of the Fe-N-C catalyst could also be measured by STS. Fig. 4e shows the STS spectrum taken on GN, which gave no distinct peaks at near the Fermi level. However, dI/dV spectrum over the bright dot gave a sharp peak at about −630 meV below the Fermi level. Macrocycle molecules with the FeN_4 center, e.g. FePc, usually have a large gap between their highest occupied molecular orbital (HOMO) and the lowest unoccupied molecular orbital (LUMO). Consequently, when deposited on graphene, the adsorbed molecule typically exhibits sharp electronic states, corresponding to their HOMO and LUMO levels, which are 1.5–2 eV away from the Fermi level. In Fig. 4e, the sharp resonance state at −0.63 eV below the Fermi level indicates that an isolated FeN_x center strongly interacts with the graphene lattice and introduces a new electronic state, which does not come from N doping or adsorbed FePc molecules [17,18]. DFT calculation suggested that an FeN_4 moiety was embedded into the GN (Fig. 4f), resulting the molecular-orbital-like peak structure in the dI/dV spectra (Fig. 4e). Compared with the large gap between HOMO and LUMO in FePc molecules, the calculated density of states (Fig. 5) show a few resonance states of Fe 3*d* at 0.4–0.8 eV below the Fermi level and a sharp resonance state at 0.2 eV above the Fermi level.

We have also investigated the edge structure of these GNs and found no decoration of metallic clusters or centers (Fig. 6). Note that high energy vacancies or defects, such as carbon vacancies [19] and pentagon-heptagon pairs [20], were rarely observed on GN. Previous studies have expected that ball milling would introduce more defects to graphene sheets while reducing their size [13]. Our studies show that, other than the increase of edge densities and edge functionalization, ball milling does not promote the formation of high energy vacancies in the planar surface. The functionalization of edges of GN was also not obvious from AFM or STM images, which explains the poor solubility of our catalysts in the polar solvents. Combining AFM and STM, we obtained local atomic structure of the Fe-N-C catalyst and verified the functionalization

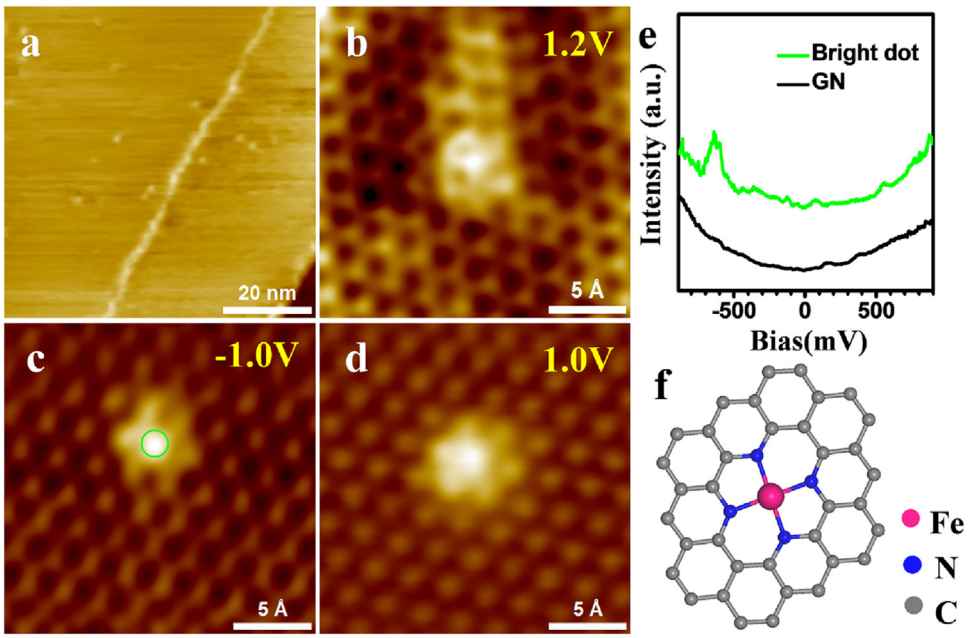

Fig. 4. The structure and electronic property of the Fe-N-C catalyst on HOPG. (a) Large scale STM image of the Fe-N-C catalyst with image size at 70 nm × 70 nm. (b) Atomic resolution STM image of the Fe-N-C catalyst, i.e. FeN_x species embedded in the GN matrix. (c) and (d) display the atomic structure of the Fe-N-C catalyst at different bias conditions. Scanning parameters: (c) Us = −1.0 V, I = 0.3 nA, (d) Us = 1.0 V, I = 0.2 nA. The center bright spot and neighboring atomic spots were enlightened, regardless the bias polarity. STS spectra taken on GN and at the bright dot of the GN were displayed in (e). The atomic structure of bright dot has been attributed by DFT calculations as the FeN_4 moiety embedded in the graphene matrix, whose structure is illustrated in (f).

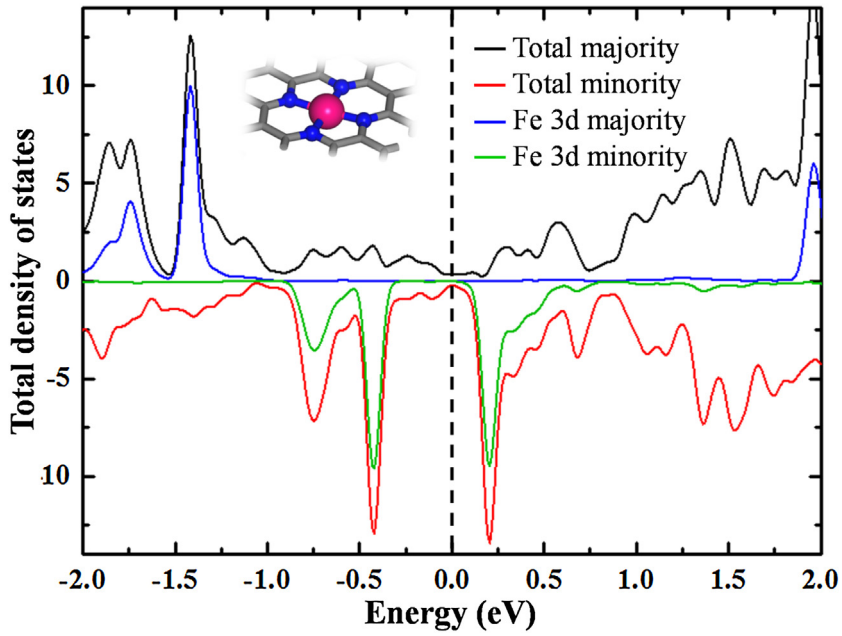

Fig. 5. Calculated density of states of the Fe-N-C catalyst. Spin polarization is included in the calculation and the Fermi level is aligned at 0 eV. The structural model is proposed as the FeN_4 moiety embedded into the graphene skeleton. Fe, N and C atoms are represented by pink, blue balls and black sticks, respectively. (For interpretation of the references to colour in this figure legend, the reader is referred to the web version of this article.)

of GN via ball milling methods. Our study thus provides not only an atomic insight to the Fe-N-C catalyst, but also a procedure for the atomic characterization of powder catalysts using surface science approach.

4. Conclusion

Combining AFM (operated in air) and STM (operated in UHV), we described a procedure that enables the atomic characterization of powder catalyst. Using the Fe-N-C catalyst as an example, we demonstrated that the selection of solvent is key to the homogeneous dispersion of powder catalyst on a planar support, which subsequently enables atomic characterization by UHV STM. The Fe-N-C catalyst, as a GN-based nanomaterial, can be homogeneously dispersed onto HOPG by a solvent of low polarity, such as petroleum ether, but did not disperse well by polar solvent, such as methanol. GN, when deposited from the solution, grew homogeneously on HOPG, indicating a weak interaction among GN. Local atomic and

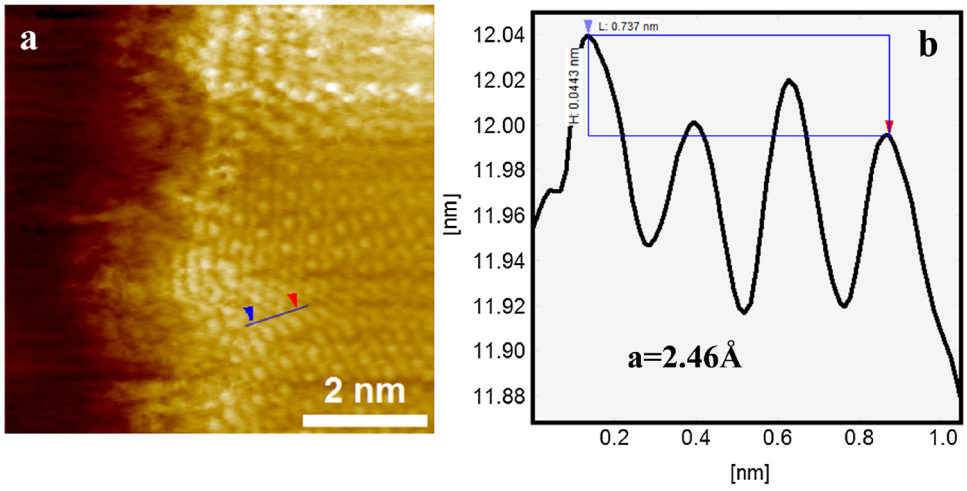

Fig. 6. STM image on the edge structure of the Fe-N-C catalyst. No decoration of metal clusters was found at the edge. Image size of (a) is 7 nm × 7 nm and scanning parameters are: Us = 0.1 V, I = 3.6 nA. Since the step edge interacts with the STM tip during scanning, distorted rows caused by tip change were observed at the top part of (a). The lattice spacing was measured at the bottom part of (a), which displays a hexagonal lattice. (b) shows the line profile marked by the bule line in (a) and displays a lattice spacing of ~2.46 Å.

electronic structure of the Fe-N-C catalyst could be obtain by STM and STS. In combination with theoretical calculations, the results suggested the FeN_4 moiety was embedded into the graphene lattice via ball milling, which provides an insight for the use of ball milling in the functionalization of two dimensional materials.

Acknowledgments

This work was financially supported by Natural Science Foundation of China [21473191, 21303195 and 91545204]; Ministry of Science and Technology of China [2013CB933100 and 2016YFA0202803] and Strategic Priority Research Program of the Chinese Academy of Sciences [XDB17020200].

References

[1] D. Deng, X. Chen, L. Yu, X. Wu, Q. Liu, Y. Liu, H. Yang, H. Tian, Y. Hu, P. Du, R. Si, J. Wang, X. Cui, H. Li, J. Xiao, T. Xu, J. Deng, F. Yang, P.N. Duchesne, P. Zhang, J. Zhou, L. Sun, J. Li, X. Pan, X. Bao, A single iron site confined in a graphene matrix for the catalytic oxidation of benzene at room temperature, Sci. Adv. 1 (2015) e1500462.
[2] X. Guo, G. Fang, G. Li, H. Ma, H. Fan, L. Yu, C. Ma, X. Wu, D. Deng, M. Wei, D. Tan, R. Si, S. Zhang, J. Li, L. Sun, Z. Tang, X. Pan, X. Bao, Direct, nonoxidative conversion of methane to ethylene, aromatics, and hydrogen, Science 344 (2014) 616–619.
[3] B. Qiao, A. Wang, X. Yang, L.F. Allard, Z. Jiang, Y. Cui, J. Liu, J. Li, T. Zhang, Single-atom catalysis of CO oxidation using Pt1/FeOx, Nat. Chem. 3 (2011) 634–641.
[4] F. Yang, E. Trufan, R.D. Adams, D.W. Goodman, Structure of molecular-sized Ru_3Sn_3 clusters on a SiO_2 film on Mo(112), J. Phys. Chem. C 112 (2008) 14233–14235.
[5] X.-F. Yang, A. Wang, B. Qiao, J. Li, J. Liu, T. Zhang, Single-atom catalysts: a new frontier in heterogeneous catalysis, Acc. Chem. Res. 46 (2013) 1740–1748.
[6] J. Masa, W. Xia, M. Muhler, W. Schuhmann, On the role of metals in nitrogen-doped carbon electrocatalysts for oxygen reduction, Angew. Chem. Int. Ed. 54 (2015) 10102–10120.
[7] R.V. Jagadeesh, A.-E. Surkus, H. Junge, M.-M. Pohl, J. Radnik, J. Rabeah, H. Huan, V. Schünemann, A. Brückner, M. Beller, Nanoscale Fe_2O_3-based catalysts for selective hydrogenation of nitroarenes to anilines, Science 342 (2013) 1073–1076.
[8] S.R. Stoyanov, A.V. Titov, P. Král, Transition metal and nitrogen doped carbon nanostructures, Coord. Chem. Rev. 253 (2009) 2852–2871.
[9] F.A. Westerhaus, R.V. Jagadeesh, G. Wienhöfer, M.-M. Pohl, J. Radnik, A.-E. Surkus, J. Rabeah, K. Junge, H. Junge, M. Nielsen, A. Brückner, M. Beller, Heterogenized cobalt oxide catalysts for nitroarene reduction by pyrolysis of molecularly defined complexes, Nat. Chem. 5 (2013) 537–543.
[10] W. Liu, L. Zhang, W. Yan, X. Liu, X. Yang, S. Miao, W. Wang, A. Wang, T. Zhang, Single-atom dispersed Co-N-C catalyst: structure identification and performance for hydrogenative coupling of nitroarenes, Chem. Sci. 7 (2016) 5758–5764.
[11] S.L. James, C.J. Adams, C. Bolm, D. Braga, P. Collier, T. Friscic, F. Grepioni, K.D.M. Harris, G. Hyett, W. Jones, A. Krebs, J. Mack, L. Maini, A.G. Orpen, I.P. Parkin, W.C. Shearouse, J.W. Steed, D.C. Waddell, Mechanochemistry: opportunities for new and cleaner synthesis, Chem. Soc. Rev. 41 (2012) 413–447.
[12] S.L. Craig, Mechanochemistry: a tour of force, Nature 487 (2012) 176–177.
[13] D. Deng, L. Yu, X. Pan, S. Wang, X. Chen, P. Hu, L. Sun, X. Bao, Size effect of graphene on electrocatalytic activation of oxygen, Chem. Commun. 47 (2011) 10016–10018.
[14] D. Tománek, S.G. Louie, First-principles calculation of highly asymmetric structure in scanning-tunneling-microscopy images of graphite, Phys. Rev. B 37 (1988) 8327–8336.
[15] D. Pandey, R. Reifenberger, R. Piner, Scanning probe microscopy study of exfoliated oxidized graphene sheets, Surf. Sci. 602 (2008) 1607–1613.
[16] S. Deng, V. Berry, Wrinkled, rippled and crumpled graphene: an overview of formation mechanism, electronic properties, and applications, Mater. Today 19 (2016) 197–212.
[17] T.G. Gopakumar, T. Brumme, J. Kroger, C. Toher, G. Cuniberti, R. Berndt, Coverage-driven electronic decoupling of Fe-phthalocyanine from a Ag(111) substrate, J. Phys. Chem. C 115 (2011) 12173–12179.
[18] A. Mugarza, R. Robles, C. Krull, R. Korytar, N. Lorente, P. Gambardella, Electronic and magnetic properties of molecule-metal interfaces: transition-metal phthalocyanines adsorbed on Ag (100), Phys. Rev. B 85 (2012) 155437.
[19] M.M. Ugeda, D. Fernandez-Torre, I. Brihuega, P. Pou, A.J. Martinez-Galera, R. Perez, J.M. Gomez-Rodriguez, Point defects on graphene on metals, Phys. Rev. Lett. 107 (2011) 116803.
[20] H. Yan, C.-C. Liu, K.-K. Bai, X. Wang, M. Liu, W. Yan, L. Meng, Y. Zhang, Z. Liu, R.-f. Dou, J.-C. Nie, Y. Yao, L. He, Electronic structures of graphene layers on a metal foil: the effect of atomic-scale defects, Appl. Phys. Lett. 103 (2013) 143120.